High-harmonics and isolated attosecond pulses from MgO

Zahra Nourbakhsh,[1] Nicolas Tancogne-Dejean,[1] Hamed Merdji,[2] and Angel Rubio[1,3,4]

[1] *Max Planck Institute for the Structure and Dynamics of Matter, Luruper Chaussee 149, 22761 Hamburg, Germany.*
[2] *LIDYL, CEA, CNRS, Universit Paris-Saclay,CEA Saclay 91191 Gif sur Yvette, France*
[3] *Nano-Bio Spectroscopy Group and ETSF, Departamento de Fisica de Materiales, Universidad del País Vasco UPV/EHU, 20018, San Sebastián, Spain.*
[4] *Center for Computational Quantum Physics (CCQ), The Flatiron Institute, 162 Fifth Avenue, New York, New York 10010, USA.*

Supplementary Note 1: Impact of the bandgap correction on HHG and IAP

Since DFT calculations in LDA or GGA (generalized gradient approximation) levels underestimate the bandgap; we employ the TB09 meta-GGA functionals, which yields an accurate estimation of MgO bandgap, to see the impact of the bandgap correction on HHG and IAP for the pulse characteristic displayed in Fig. S2a. The results presented in Fig. S1 imply that the gap enhancement does not affect our main results; however, it weakens the HHG as well as IAP intensities for an order of magnitude, which can be easily understood in terms of a decreased ionization, as we opened the bandgap of MgO.

Supplementary Note 2: Impact of the pulse intensity on HHG and IAP

The HHG spectra of the two-color pulses introduced in the main part are shown in Fig. S2. The electric-field strength increases from right to left.

It should be noted that the band structure has an important role to analyze the high-harmonics emission in solids; because of the discrete band structure in solids, the cutoff energy definition for a HHG spectrum corresponding to a solid target is not as clean as that in gases. It is possible to define several cutoff energies in a HHG spectrum obtained from a solid. We consider the cutoff energy as the spectral position where the intensity decreases by an order of magnitude at a given harmonic and beyond, averaged over a large bandwidth of several eV.

In order to evaluate the effect of driving pulse intensity in IAP generation, Fig. S4 presents one-color pulses HHG spectra. Here, the harmonic emissions are controlled just by the pulse intensity; the second pulse frequency is same as the fundamental pulse, and its phase is set to zero. In Fig. S4 from left to right, the pulse intensities are respectively six, four, and two times the fundamental pulse intensity. This calculation clearly reveals that with an appropriate spectral filtering, IAPs can effectively be produced and optimized with the pulse intensity enhancement. As shown in the main text, no IAP is generated from the fundamental pulse while the intensity enhancement makes it possible. This result is in contrast to what we concluded from two-color pulses. Since the intensity does not play any explicit role in the IAP, generated by the two-color pulse (shown in Fig. S2); it reveals the strong impact and importance of asymmetric pulses in IAP generation. In addition, the two-color IAPs are much shorter and brighter than those achieved from the one-color laser. Regarding their wider energy window, they also show more flexibility compared to one-color-based IAP.

Figure S5 shows the cutoff energy evolution as a function of the maximum value of the driving pulse electric-field strength; this plot exhibits that the cutoff energy increases with the electric-field enhancement. Regarding Fig. S5, the cutoff energies corresponding to the pulses with the same wavelength rise linearly as a function of the electric-field strength. But for the two-color pulses, with mixed wavelengths, the cutoff energies are not located on this line, and they have a lower value. Since our results predict that cutoff energy is not dependent on the wavelength (not shown), this shows the impact of non-symmetric pulse beating.

Supplementary Note 3: Impact of the ionic potential on HHG

The impact of the gradient of the electron-nuclei potential in HHG is discussed in Ref. [1]; it is shown that

$$HHG \propto \left| FT\Big(\int_\Omega d\mathbf{r}\; n(\mathbf{r},t) \nabla v_{\mathrm{nuc}}(\mathbf{r}) \Big) + N_e \mathbf{E}(\omega) \right|^2, \quad (1)$$

where $v_{\mathrm{nuc}}(\mathbf{r})$ is the electron-ion potential, N_e the number of electrons and $\mathbf{E}$ the driving electric field. Obviously the second term does not lead to non-perturbative harmonics, and thus the term $\nabla v_{\mathrm{nuc}}(\mathbf{r})$ plays a key role in the harmonic emission. Since the [100] direction in MgO is along the Mg-O ionic bonds, $\nabla v_{\mathrm{nuc}}(\mathbf{r})$ in this direction has its largest value, and it is therefore expected to have a stronger emission for light polarization along the [100] direction comparing to other directions.

Supplementary Note 4: Impact of the second pulse rotation on HHG

Fig. S6 displays the two-color HHG spectrum as a function of the second pulse rotation angle as well as

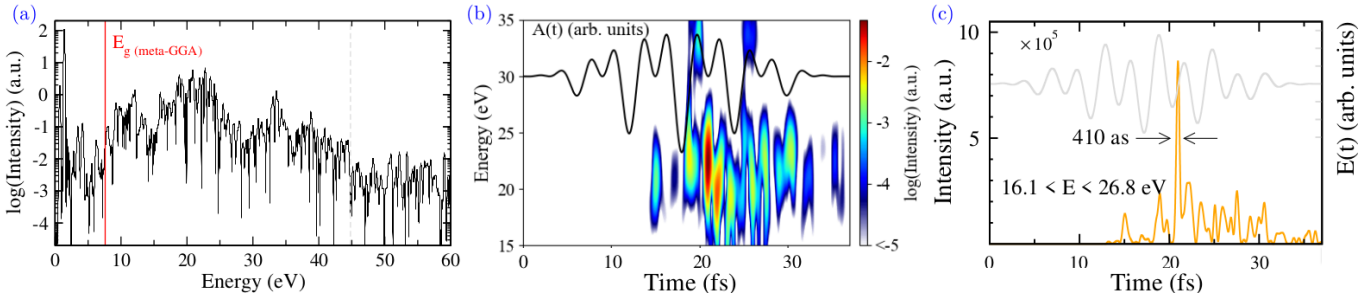

FIG. S1. The meta-GGA calculation results. (a) HHG spectrum corresponding to the pulse characteristics displayed in Fig. S2a; the pulse polarization is along the [100] direction. The dashed gray line marks the cutoff energy. The solid red line indicates the MgO bandgap obtained at the meta-GGA level which is equal to 7.6 eV. (b) Time-frequency analysis of the HHG. The time window to calculate the Gabor transform is taken to be 0.25 fs. This figure also shows the time profile of the vector potential. (c) The resulted attosecond pulse for the given energy window.

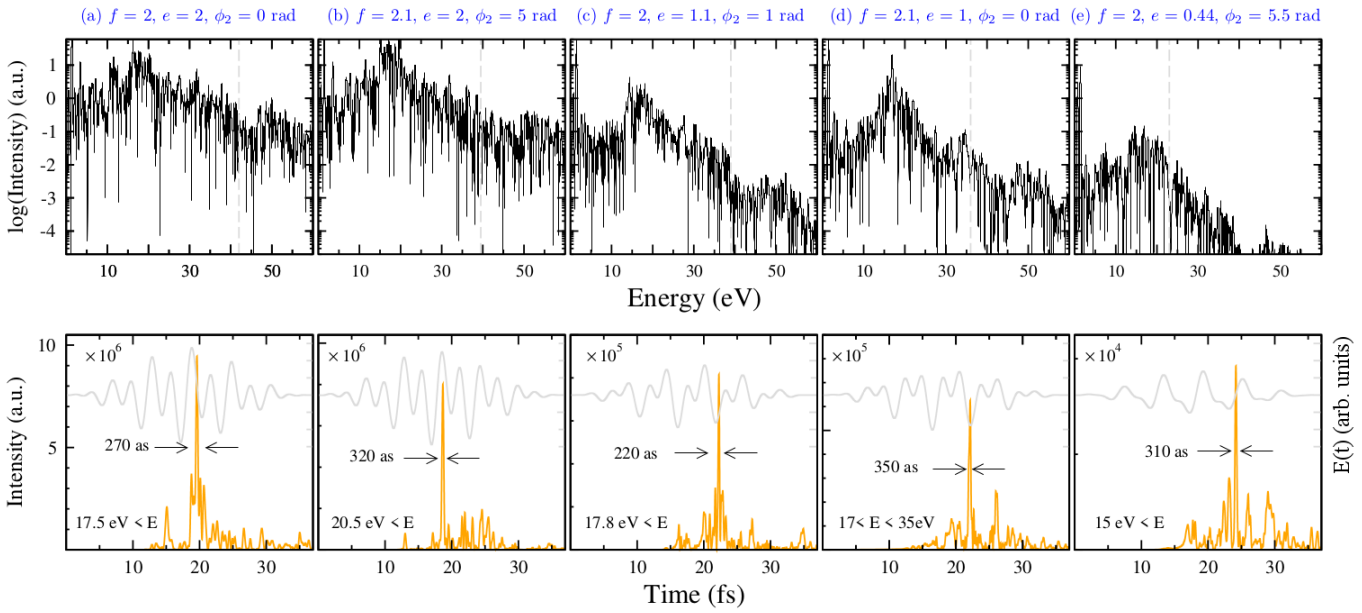

FIG. S2. Calculated HHG spectra (top row) and their related IAPs (bottom row) for different two-color pulses. The titles specify the pulse characteristics; e, f and ϕ_2 as defined in Eq. 5 in the main text. The light polarization is along the [100] direction. The gray dashed lines in the HHG spectra mark the cutoff energies. The IAP duration and the corresponding energy windows are given in the bottom panels. The total electric-field profiles are also shown in light gray in the bottom row, using the same scale for the panels.

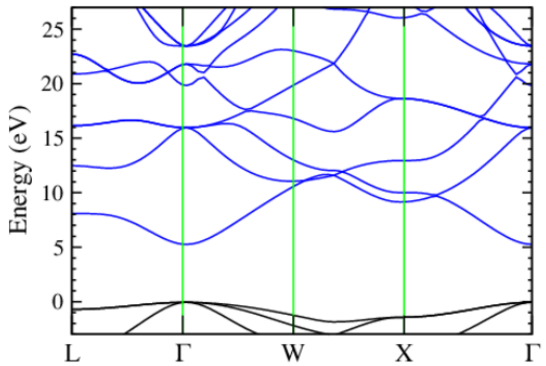

FIG. S3. Bulk MgO DFT-LDA band structure. It is shown in the fcc lattice high symmetry path; the valence (conduction) bands are in black (blue). The top of the valence band is set to be zero.

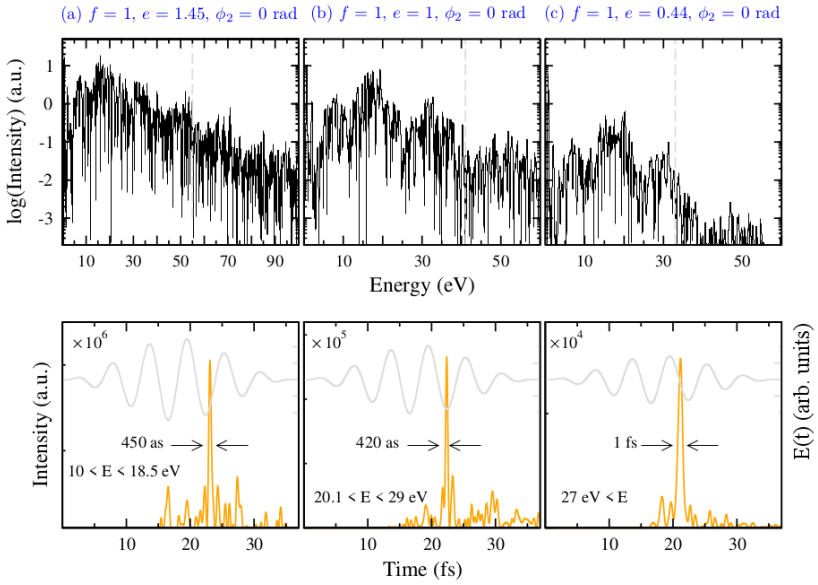

FIG. S4. Impact of the pulse intensity on high-harmonics and IAP generation for the case of one-color pulse. The pulse characteristics are the same as the fundamental laser pulse, but from the right to the left, the pulse intensities are respectively $2I_0$, $4I_0$ and $6I_0$ where I_0 is the fundamental pulse intensity.

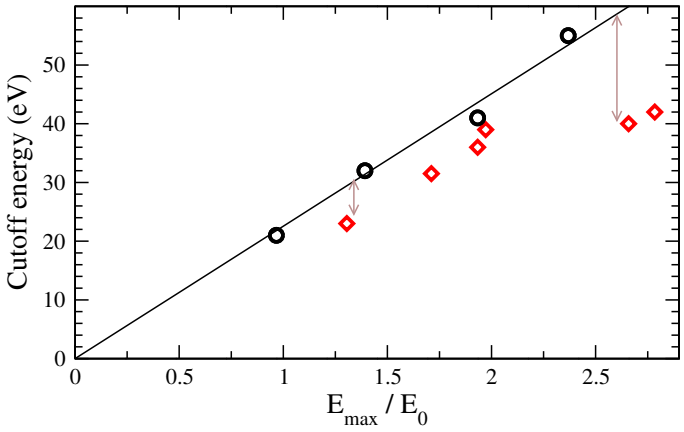

FIG. S5. Harmonic cutoff energies as a function of their electric-field maximum. The points are for the reported pulses in Figs. S2 and S4 as well as the fundamental pulse. E_0 and E_{max} denote the fundamental and the related pulse maximum electric field, respectively. The black circles (red diamonds) relate to the one (two) color pulses. The brown arrows show that the same electric fields could lead to different cutoff energies which reveals the impact of the two color beating. Regarding to e and ϕ_2 parameters defined in the paper and Figs. S2 and S4, if $\phi_2 = 0$, $E_{max}/E_0 = 1 + e$.

the polarization resolved HHG spectra. The x-polarized HHG (HHGx) offers a declining trend *versus* the second pulse rotation while the y-polarized HHG (HHGy) reaches its maximum around $\theta = 45°$; it means that for $45° < \theta < 90°$, HHGy is a decreasing function of E_y which implies the effect of E_x in y-polarized harmonics. Figure S7 gives another example of this behavior. This figure compares HHGx when the second applied pulse is rotated of 90° and the HHG resulting from the fundamental laser pulse only (as already shown in Fig. 1 in the main text). Since for both cases, the x component of the total electric fields is identical, this figure reveals the role of the E_y in enhancing the emission along the x direction. This behavior is compatible with what is expected from an elliptically polarized pulse in solids regarding the extended valence hole which strengthens the ellipticity response of solids; additionally, it could make sense as the vertical electric field, here the component of the pulse along the y, could ionize the system and make the HHG process easier.

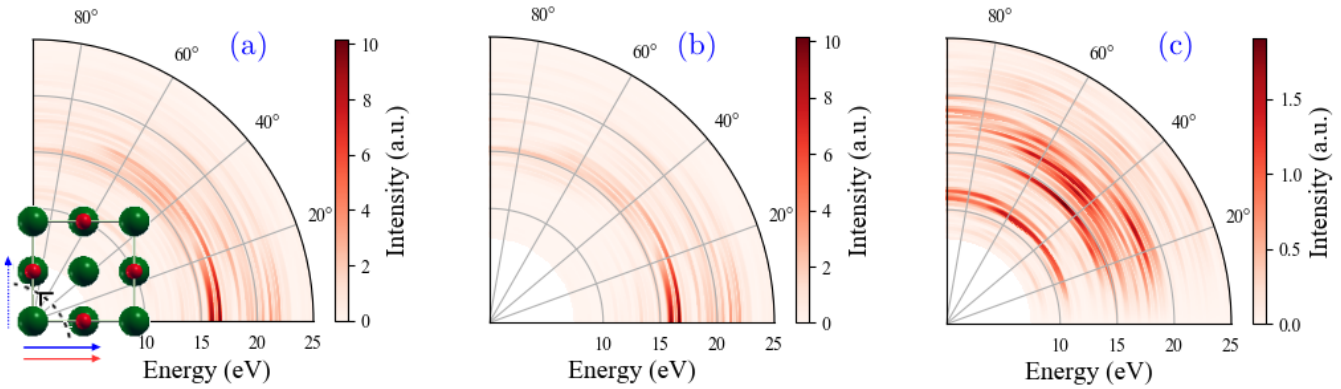

FIG. S6. Two-color pulse HHG spectra as a function of the second field polarization direction. The contour displayed in (a) shows the total HHG while (b) and (c) respectively indicate the high-harmonic spectra/emission with polarization along x and y directions (HHGx and HHGy). The first field polarization is fixed along the [100] direction. Note that the intensity scales are linear. The HHG with x polarization, namely HHGx, is stronger than HHGy.

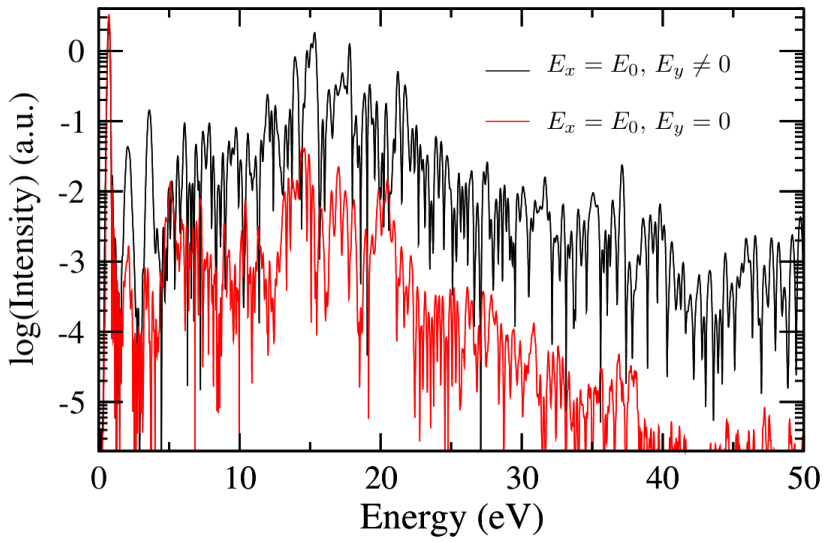

FIG. S7. Comparison between x-polarized HHG (HHGx) of two different pulses with the same electric fields in x-direction. Red shows the fundamental pulse HHG (also displayed in Fig. 1) and the black is the x-polarized HHG of the pulse displayed in Fig. S6 when the second field polarization is along y direction.

[1] N. Tancogne-Dejean, O. D. Mücke, F. X. Kärtner, A. Rubio, Impact of the electronic band structure in high-harmonic generation spectra of solids, Phys. Rev. Lett. **118**, 087403 (2017).